Modeling Carbon Dioxide Adsorption on Microporous Substrates: Comparison between Cu-BTC Metal−Organic Framework and 13X Zeolitic Molecular Sieve

Paolo Aprea,[†] Domenico Caputo,[†] Nicola Gargiulo,[†] Fabio Iucolano,[†] and Francesco Pepe*[,‡]

Dipartimento di Ingegneria dei Materiali e della Produzione, Università Federico II, P.le Tecchio 80, 80125 Napoli, Italy, and Dipartimento di Ingegneria, Università del Sannio, P.zza Roma 21, 82100 Benevento, Italy

In this work, CO_2 adsorption on a laboratory-synthesized polymeric copper(II) benzene-1,3,5-tricarboxylate (Cu-BTC) metal−organic framework was modeled by means of the semiempirical Sips equation in order to obtain parameters of engineering interest. Produced Cu-BTC samples were characterized by X-ray diffraction, thermogravimetry, and microporosimetric analysis; high crystallinity and very high specific surface area and pore volume were found. CO_2 adsorption isotherms on Cu-BTC were evaluated at $T =$ (283, 293, 318, and 343) K for $p \leq 1$ bar by means of a volumetric technique. In order to establish a comparison, CO_2 adsorption isotherms on samples of commercial 13X zeolite were determined under the same experimental conditions and then modeled in the same way as those for Cu-BTC. The modeling and experimental results indicated that relative to 13X zeolite, Cu-BTC showed higher CO_2 adsorption capacities at near-ambient temperature and a lower heat release during the adsorption phase.

1. Introduction

Carbon dioxide (CO_2) is the most relevant contributor to the greenhouse effect. However, more than 10 years after the Kyoto protocol (1997), emissions of CO_2 and other greenhouse gases continue to increase.[1] Therefore, it is necessary to set up adequate technologies to avoid CO_2 production in the first place and to avoid its release into the atmosphere when no alternatives to its production exist. Anthropogenic CO_2 emissions are mainly due to combustion processes, even though a number of other industrial processes, such as hydrogen production, give significant contributions.[2] One possible way to avoid CO_2 emissions from these processes is to remove this species from the gaseous streams in which it is contained in order to safely dispose of it in deep underground areas, such as exhaust oil reservoirs or ocean sediments. Moreover, it is important to observe that the issue of CO_2 removal from a gaseous stream arises in other situations apart from control of CO_2 release into the atmosphere. Examples in this sense are the processes for cryogenic air separation and NH_3 synthesis. Indeed, in cryogenic air separation plants, air sent to liquefaction must be de facto CO_2-free; otherwise, a blockage due to freezing in the heat exchange equipment could result.[3] Similarly, in NH_3 synthesis by the reaction between H_2 and N_2, CO_2 is present in very large amounts in the H_2 stream, and its concentration must be reduced to parts per million levels in order to avoid problems with the synthesis reactor.[3]

CO_2 removal from gaseous streams has historically been carried out by physical or chemical absorption using aqueous solvents such as moderately concentrated amine solutions or potassium carbonate solutions. An important alternative technology is represented by adsorption, usually carried out as pressure-swing adsorption (PSA) or sometimes as vacuum-swing adsorption (VSA). The materials more often considered for PSA/VSA processes have been microporous adsorbents, which are characterized by pores having sizes of less than 2 nm free diameter. Among these, both traditional adsorbing materials (e.g., silica gel, activated alumina, and activated carbon) and aluminosilicates of the class of zeolites have been considered.[4] In particular regard to zeolites, by appropriate choices of framework structure, Si/Al ratio, and extraframework cationic content, it is possible in certain cases to tailor the adsorptive properties to achieve the selectivity required for a particular separation.[4] 13X zeolite, which is characterized by a relatively high surface basicity, has been shown to be a very suitable adsorbent for CO_2 capture by PSA processes.[5] Despite the wide use of zeolites for CO_2 capture, active research efforts during the last two decades have been devoted to adsorption-based CO_2 separation processes, and more specifically to the selection of novel, more selective adsorbents, since the development of such adsorbents has the potential to greatly improve the performance of the adsorption process. In recent years, the use of functionalized mesostructured silicas as adsorbents for CO_2 separation has been widely investigated,[6−11] with particular focus on so-called "molecular baskets", which consist of mesoporous silicas functionalized with polyethylenimine (PEI) chains.[12] These materials have a noticeable tendency to reach saturation even at very low values of CO_2 partial pressure (chemisorption-type behavior) and therefore appear to be particularly suitable for separation processes in which complete CO_2 removal justifies the use of absolute pressure on the order of 10^{-6} bar for sorbent regeneration but not for standard PSA/VSA processes.[13] More recently, several adsorbent materials belonging to the class of microporous metal−organic frameworks (MOFs) have proven to be good candidates for improving the performance of adsorption-based CO_2 sequestration processes. MOFs are hybrid materials in which metal ions or small metallic nanoclusters are linked into one-, two-, or three-dimensional structures by multifunctional organic linkers. The most interesting feature of MOFs is their extremely high specific surface area,[14] which can reach values as high as 6000 $m^2 \cdot g^{-1}$. Several MOFs have been

* Corresponding author. Telephone: +390824305589. Fax: +390824325246. E-mail: francesco.pepe@unisannio.it.
[†] Università Federico II.
[‡] Università del Sannio.

10.1021/je1002225
Published on Web 07/19/2010

proposed as adsorbents for CO_2 separation processes,[15] and among these are MIL-47 [polymeric vanadium(IV) benzene-1,4-dicarboxylate], MIL-53 [porous chromium(III) benzene-1,4-dicarboxylate], and Cu-BTC [polymeric copper(II) benzene-1,3,5-tricarboxylate]. In particular, MIL-47 showed good CO_2 adsorption capacity,[16] while MIL-53 showed a very high selectivity for CO_2 over CH_4[17] and Cu-BTC proved to have noticeable CO_2 adsorption capacity and selectivity relative to N_2.[18] Chowdhury and co-workers[19] compared CO_2 adsorption isotherms on Cu-BTC samples synthesized via different routes and showed that two different scaling factors (one for low levels of adsorbent loading and another for high levels) can be employed to match isotherms obtained using samples with significant differences in specific surface areas and pore volumes. On the other hand, Liang and co-workers[20] compared the CO_2 adsorption performance of laboratory-synthesized Cu-BTC and commercial 13X zeolite and found that Cu-BTC showed a much higher CO_2 working capacity, which is defined as the difference between the CO_2 adsorption capacities determined for the high and low pressures of interest in a PSA separation process.

In the light of the results presented by Liang and co-workers, the aim of the present work is to deepen such a comparison by employing a suitable model for obtaining parameters of engineering interest from experimental CO_2 adsorption isotherms on the aforementioned two substrates. The isotherms were obtained at four different temperatures between (283 and 343) K at pressures up to 1 bar, taking into account the fact that the CO_2 concentration in gas streams of engineering interest (e.g., flue gas) rarely leads to a partial pressure significantly higher than 1 bar. The experimental data were then processed by means of the semiempirical Sips model to find the values of the isosteric heat of adsorption (i.e., the ratio of the infinitesimal change in the adsorbate enthalpy to the infinitesimal change in the amount adsorbed) and other relevant parameters such as CO_2 affinity and maximum adsorption capacity.

2. Experimental Section

Cu-BTC samples were obtained as powders using a procedure described by Wang and co-workers:[18] 2.46 g (11.7 mmol) of benzene-1,3,5-tricarboxylic acid (Aldrich) was dissolved in 13 mL of ethanol (Baker), and 5.43 g (23.3 mmol) of copper nitrate hydrate (Baker) was dissolved in 13 mL of doubly distilled water. The two solutions were then mixed at ambient temperature and aged for 30 min, after which the resulting mixture was heated at 383 K under solvothermal conditions for 18 h. The reaction vessel was allowed to reach ambient temperature, and the resulting blue crystals were isolated by filtration and washed with doubly distilled water. The final product was then dried at 383 K overnight.

Powder X-ray diffraction (XRD) patterns of Cu-BTC samples were collected using a Philips PW1710 apparatus with Cu $K\alpha_1$ radiation. The scanning step size was 0.020° in 2θ, and the time for each step was 1 s. In light of the well-known sensitivity to moisture that characterizes Cu BTC,[18] the XRD pattern was obtained while taking special care to minimize water adsorption by the samples to be analyzed, and with this aim, the dried samples were exposed to ambient air for a minimal amount of time. Unit cell constants were calculated using the McMaille 4.00 software package starting from the 20 most significant diffraction peaks. Scanning electron microscopy (SEM) micrographs were collected with a Cambridge S440 instrument, while thermogravimetric (TG) analysis was carried out with a Netzsch STA 409 Luxx device using samples with masses of about 0.020 g that were heated in an air flow from ambient temperature up to 673 K at a rate of 10 $K \cdot min^{-1}$ and using α-alumina as reference. Microporosimetric characterization was carried out by N_2 adsorption/desorption cycles at 77 K, and the specific surface area was evaluated by means of the Brunauer−Emmett−Teller (BET) method. A Micromeritics ASAP 2020 volumetric instrument was used for this purpose, and synthesized samples were degassed at 423 K for 3 h prior to characterization.

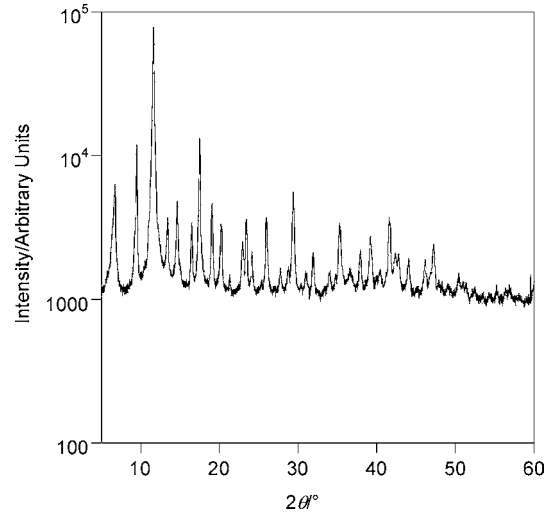

Figure 1. Powder XRD pattern of synthesized Cu-BTC.

CO_2 adsorption isotherms on Cu-BTC and 13X zeolites were obtained using the ASAP 2020 instrument mentioned above. However, since ASAP-series devices were mainly designed to work at the boiling temperatures of noble/inert gases, the Dewar flask in which the sample tube is usually immersed was substituted by an "ad hoc" container whose shell was filled with flowing thermostatted water. 13X zeolite samples used for adsorption experiments were supplied by Carlo Erba (Italy) and used as purchased. Prior to each adsorption experiment, Cu-BTC samples were degassed under high vacuum at 423 K for 3 h, while for 13X samples, because of their greater thermal stability, a degassing temperature of 573 K was chosen. Since no preliminary data about the CO_2 adsorption kinetics on the adsorbent samples synthesized in this work were available, each adsorption step was allowed to approach equilibrium over a period of (1 to 2) h in order to collect isotherm points that could be reliably considered as depictive of an equilibrium state. Adsorption isotherms were obtained at four different temperatures, namely, T = (283, 293, 318, and 343) K. N_2 adsorption isotherms for both Cu-BTC and 13X were also obtained at T = 293 K.

3. Results

3.1. Characterization of Synthesized Cu-BTC. The XRD pattern of synthesized Cu-BTC, which is shown in Figure 1, is consistent with those reported by previous workers.[18] The noticeably strong intensity of peaks in the pattern can usually be related to the formation of large crystals, but in this case it might also be related to the low water content inside the pore structure of the sample itself.[21] This in turn depends on the fact that, as mentioned above, the analyzed sample was introduced into the analysis chamber immediately after the drying process at 383 K. The refinement of the diffraction pattern indicated that synthesized Cu-BTC crystals have cubic symmetry with a unit cell constant of 26.313 Å. Such results are fairly comparable with those reported by Chui and co-workers,[22] who registered the same symmetry and a unit cell constant of 26.343 Å.

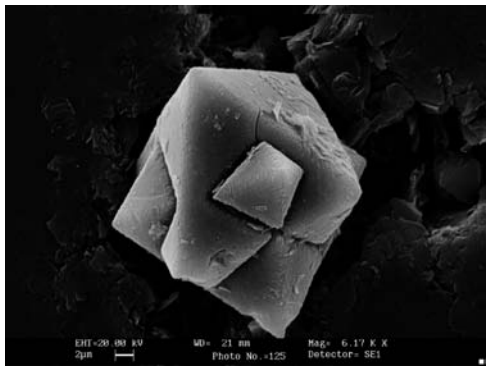

Figure 2. SEM micrograph of synthesized Cu-BTC crystals.

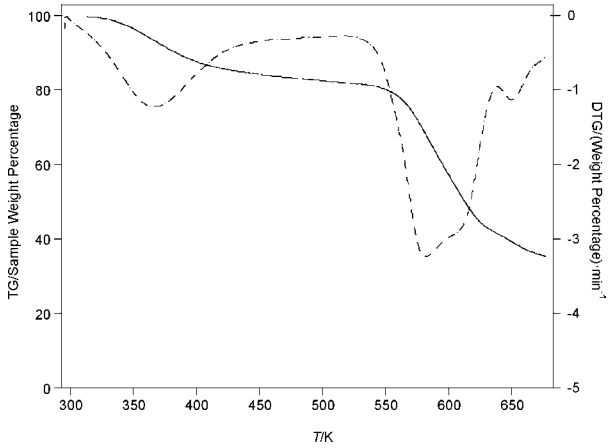

Figure 3. Thermogravimetric (TG) analysis curve (solid) and differential thermogravimetric (DTG) analysis curve (dot-dashed) of synthesized Cu-BTC.

Figure 2 shows a SEM micrograph of synthesized Cu-BTC: although the large particle shown in the figure is clearly polycrystalline, the reported image is consistent with the indications deriving from inspection of Figure 1 regarding the strong crystallization process that occurs during MOF-phase synthesis. The morphology of the cubic-shaped particle is also consistent with other SEM investigations performed on Cu-BTC.[18,23]

Figure 3 shows the results of TG analysis of synthesized Cu-BTC and highlights two main weight losses. The first loss registered in Figure 3 occurs at a temperature of about 370 K and is ascribable to water desorption phenomena. The second weight loss, which occurs between (570 and 630) K with a more pronounced extent than the first one, is due to the decomposition of the framework, which probably proceeds by partial combustion of benzenetricarboxylate moieties and formation of copper oxides.[21]

Figure 4 shows N_2 adsorption/desorption isotherms on synthesized Cu-BTC measured using the ASAP 2020 apparatus at 77 K. Quite apparently, the curve reported in Figure 4 is a type-I isotherm, which is typical of microporous materials.[24] The absence of hysteresis phenomena confirmed that the synthesized product possessed no other pore system apart from that of the micropores. At saturation, the adsorbed amount of N_2 was 19.8 mol·kg^{-1}; under the assumption that the adsorbate density is that of the liquid phase (the so-called "Gurvitch rule"),[25] multiplying by the molar volume of liquid nitrogen at 77 K (34.7 cm^3·mol^{-1}, as reported by Wang and co-workers[18]) leads to an estimated intracrystalline porosity of 0.57 cm^3·g^{-1} for Cu-BTC. This is comparable to, if not higher than, other values previously reported in the literature. For example, Wang

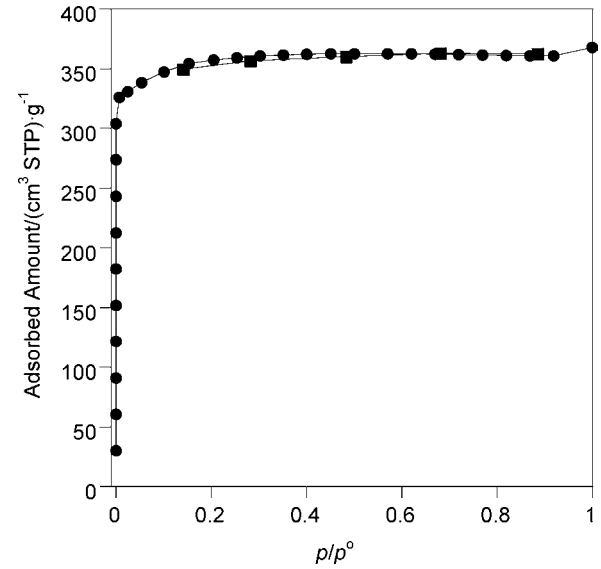

Figure 4. N_2 adsorption (●) and desorption (■) isotherms on synthesized Cu-BTC, measured using an ASAP 2020 apparatus at 77 K.

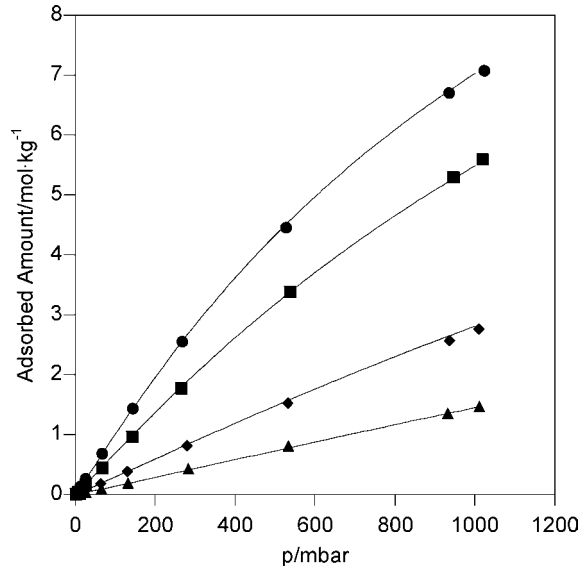

Figure 5. CO_2 adsorption isotherms on synthesized Cu-BTC, measured using an ASAP 2020 apparatus: ●, 283 K; ■, 293 K; ◆, 318 K; ▲, 343 K. Continuous lines are best-fit Sips theoretical isotherms.

and co-workers[18] reported an intracrystalline porosity of about 0.66 cm^3·g^{-1}, while Schlichte and co-workers[21] reported a value of 0.41 cm^3·g^{-1}. It must be noted that Cu-BTC samples with very high intracrystalline porosity seem to be producible only from synthesis routes that involve the use of significantly hazardous reagents such as *N*,*N*-dimethylformamide[19] or require very slow heating and cooling ramps.[20] Moreover, it is important to remark that the aforementioned value of the pore volume for Cu-BTC is more than 60% higher than that of 13X zeolite (0.35 cm^3·g^{-1}).[26] In regard to the specific surface area for synthesized samples, calculations based on the BET model led to a value of 1.40·10^3 m^2·g^{-1}, which is more than 2 times the result reported for commercial 13X (616 m^2·g^{-1}).[27]

3.2. CO_2 and N_2 Adsorption Isotherms on Cu-BTC and 13X Zeolite. Figure 5 reports CO_2 adsorption isotherms on Cu-BTC MOF at (283, 293, 318, and 343) K for CO_2 pressures ranging from (0 to 1) bar together with fits to the Sips equation (which will be analyzed in the Discussion). Figure 5 shows that over the pressure range considered, the isotherms are signifi-

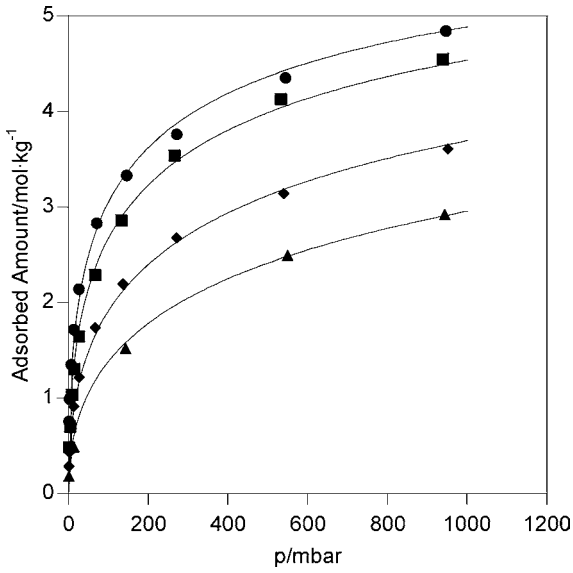

Figure 6. CO_2 adsorption isotherms on purchased 13X zeolite, measured using an ASAP 2020 apparatus: ●, 283 K; ■, 293 K; ◆, 318 K; ▲, 343 K. Continuous lines are best-fit Sips theoretical isotherms.

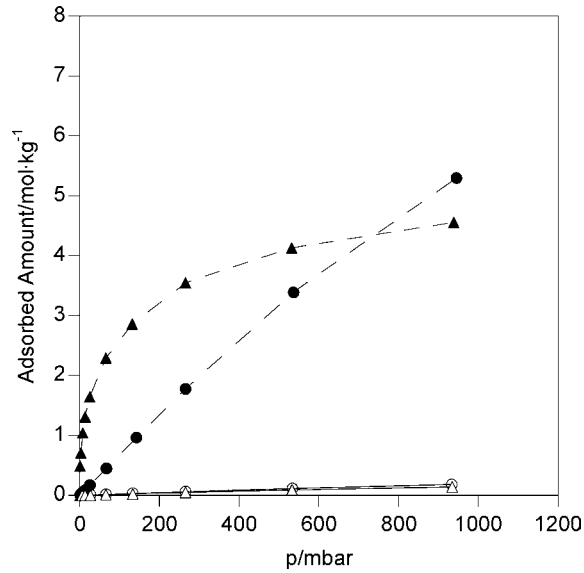

Figure 7. Adsorption isotherms of CO_2 (solid symbols, dashed lines) and N_2 (open symbols, continuous lines) on synthesized Cu-BTC (circles) and purchased 13X zeolite (triangles), measured using an ASAP 2020 apparatus at 293 K.

cantly far from their asymptotic maximum levels and show a strong pressure dependence of the amount of adsorbed CO_2. In regard to the dependence on temperature, it clearly appears that the amount of adsorbed CO_2 decreases as temperature increases, indicating that the adsorption process is exothermic. In particular, at $p = 1$ bar, the adsorbed amount q turned out to be about 7.0 mol·kg^{-1} at $T = 283$ K and about 1.5 mol·kg^{-1} at $T = 343$ K, with a ratio of about 5. It is interesting to note that over the pressure range considered in this work, the amounts of adsorbed CO_2 at 293 K are slightly higher than those at 298 K reported by Liang and co-workers.[20] Apart from the sensitivity of CO_2 adsorption capacity to temperature, this could be due to the fact that those authors used significantly lower adsorption times for each experimental point [(15 to 30) min rather than (1 to 2) h].

In order to compare the behavior of Cu-BTC with that of a more traditional microporous adsorbent, CO_2 adsorption isotherms were also determined on 13X zeolite over the same temperature and pressure ranges. The experimental results for 13X zeolite are reported in Figure 6 along with fits to the Sips equation. The isotherms reported in Figure 6 have a markedly different shape from those reported in Figure 5, with a strongly convex behavior. Also for 13X, saturation was not achieved over the pressure range explored, even though inspection of the isotherms reported in Figure 6 appears to indicate that saturation should be reached at a pressure much lower than that for Cu-BTC. Figure 6 shows that the amount of CO_2 adsorbed on 13X zeolite also decreases as the temperature increases, but in a less pronounced way than for Cu-BTC. Indeed, at $p = 1$ bar, the adsorbed amount decreased from about 4.8 mol·kg^{-1} at $T = 283$ K to about 2.9 mol·kg^{-1} at $T = 343$ K, with a ratio of about 1.6. The noticeable difference in the shapes of the CO_2 adsorption isotherms of 13X and Cu-BTC could be due to the different nature of the interactions between CO_2 molecules and the inner micropore walls of such substrates. In fact, in 13X zeolite, adsorption occurs mainly because of the slight acidity of CO_2 molecules, which enables them to interact with the slightly basic inner micropore surfaces of zeolites with a low Si/Al ratio (for 13X zeolite, the ratio is equal to 1.24). On the other hand, the nature of the interaction between CO_2 molecules and the Cu-BTC framework is completely different. In fact, the bonds between metal coordination centers and organic linkers in MOFs usually show a relevant electrostatic factor, with inorganic moieties characterized by partial positive charges. If such positively charged metal coordination centers are exposed at the inner surface of the micropores (in many cases, such as that of Cu-BTC, this can be achieved by water removal from the substrate), they can specifically interact with gas molecules having quadrupole moment different from zero, as in the case of gaseous CO_2.[20,28]

In order to verify the capability of Cu-BTC samples produced in this work with regard to CO_2 separation from other components of a gas mixture, N_2 adsorption isotherms on both Cu-BTC and 13X at 293 K were obtained using the aforementioned ASAP 2020 apparatus. Such isotherms are reported in Figure 7, together with the isotherms for CO_2 adsorption on Cu-BTC and 13X at the same temperature. Figure 7 shows that both Cu-BTC and 13X have a very low affinity for N_2, with an adsorption capacity that, at pressures of about 1 bar, is on the order of 0.15 mol·kg^{-1}, corresponding to a ratio with the similar quantity for CO_2 adsorption of close to 1/30. These results are consistent with what has already been reported by Wang and co-workers,[18] who, for example, proposed the usage of Cu-BTC for PSA processes aimed at efficient removal of CO_2 from air prior to its cryogenic distillation.

4. Discussion

In order to have a clearer understanding of the adsorption phenomena examined, a modeling effort was undertaken using the semiempirical three-parameter Sips isotherm.[29] The Sips isotherm (sometimes called the Langmuir−Freundlich isotherm) is a semiempirical model that contains mathematical aspects of both the Langmuir and Freundlich isotherms; even though its thermodynamic consistency shows limits in the very low pressure region (it does not reduce to Henry's law), its simple form does not require the definition of the saturation pressure for the adsorbate, thus making it suitable for modeling either subcritical or supercritical isotherms. According to this equation, the pressure dependence of the adsorbed amount takes the following form:

$$q = q_{max}\frac{(bp)^{1/n}}{1 + (bp)^{1/n}} \quad (1)$$

where q_{max}, n, and b are model parameters: q_{max} represents the maximum adsorption capacitiy, b is the affinity constant, and n is the heterogeneity coefficient (in particular, for $n = 1$, the Sips isotherm reduces to the Langmuir isotherm, which applies to homogeneous adsorbent−adsorbate systems). Sips parameters are in general dependent on temperature, as reported by Do,[30] but considering q_{max} and n to be independent of temperature wherever possible is strongly advisible in order to keep the model describing the system as simple as possible. For this reason, an attempt to describe CO_2 adsorption on both Cu-BTC MOF and 13X zeolite was performed by coupling eq 1 with the following expression for the description of the dependence of the affinity coefficient b on temperature:[30]

$$b = b_\infty \exp\left(\frac{Q}{RT}\right) \quad (2)$$

where b_∞ is the value of b at infinite temperature and Q is the value of the isosteric heat of adsorption when the adsorbent fractional coverage is equal to 0.5.

The experimental data concerning CO_2 adsorption on Cu-BTC and on 13X were submitted to nonlinear regression (using ad hoc scripts developed in the Matlab environment) in order to calculate simultaneously the optimal values of the parameters of eqs 1 and 2 (i.e., q_{max}, b_∞, Q, and n) for the isotherms reported in Figures 5 and 6. The calculated values of the parameters are reported in Tables 1 and 2, and the comparison between the model and the experimental results has been shown in Figures 5 and 6, in which symbols refer to experimental data and continuous curves refer to the best-fit Sips theoretical isotherms.

Inspection of Figures 5 and 6 clearly indicates a very good correlation between the model curves and the experimental points for both Cu-BTC MOF and 13X zeolite. This is also confirmed by values of the regression coefficient R^2 reported in Tables 1 and 2. Furthermore, from the analysis of the data reported in Tables 1 and 2, it can be noted that the maximum adsorption capacity q_{max} for Cu-BTC is significantly higher than that calculated for 13X zeolite (i.e., 16.5 mol·kg^{-1} vs 7.06 mol·kg^{-1}). It is interesting to observe that the calculated value of q_{max} for Cu-BTC finds a kind of validation from a comparison with the experimental results of Liang and co-workers,[20] who, commenting on the circumstance that Cu-BTC adsorbs 12.7 mol·kg^{-1} of CO_2 at 298 K and 15 bar, stated that even at such a high pressure, none of the CO_2 adsorption isotherms produced by their experimental runs appeared to have reached saturation.

In regard to the affinity coefficient b, the values of this parameter for both Cu-BTC and 13X can be calculated, for example, at $T = 293$ K by using eq 2 and the values of b_∞ and Q reported in Tables 1 and 2, respectively. Such values of b turned out to be $5.18 \cdot 10^{-4}$ mbar^{-1} for Cu-BTC and $3.48 \cdot 10^{-3}$ mbar^{-1} for 13X, thus indicating that, at ambient temperature, Cu-BTC shows a lower affinity for CO_2 than 13X does. As suggested by Siriwardane and co-workers,[5] an empirical assessment of the affinity of an adsorbent for CO_2 can be achieved by plotting adsorption isotherms as adsorbed amounts per unit area of adsorbent versus gas pressure. Figure 8 shows the CO_2 adsorption isotherms on Cu-BTC and 13X zeolite at $T = 293$ K that were already reported in Figures 5 and 6, respectively, but this time plotted in terms of adsorbed amounts per unit area. Inspection of Figure 8 clearly indicates that the number of moles

Table 1. Sips Parameters for CO_2 Adsorption on Synthesized Cu-BTC

parameter	95% confidence interval lower limit	best-fit value	95% confidence interval upper limit
q_{max}/mol·kg^{-1}	15.3	16.5	17.7
b_∞/mbar^{-1}	$9.83 \cdot 10^{-5}$	$1.25 \cdot 10^{-4}$	$1.51 \cdot 10^{-4}$
n	0.92	0.94	0.97
Q/kJ·mol^{-1}	25.5	25.9	26.3
coefficient of determination: $R^2 = 0.999$			

Table 2. Sips Parameters for CO_2 Adsorption on Purchased 13X Zeolite

parameter	95% confidence interval lower limit	best-fit value	95% confidence interval upper limit
q_{max}/mol·kg^{-1}	6.26	7.06	7.85
b_∞/mbar^{-1}	$8.81 \cdot 10^{-6}$	$5.59 \cdot 10^{-5}$	$1.03 \cdot 10^{-4}$
n	1.90	2.12	2.40
Q/kJ·mol^{-1}	30.8	32.5	34.2
coefficient of determination: $R^2 = 0.971$			

of CO_2 adsorbed per unit area of 13X zeolite is higher than that of Cu-BTC over the considered pressure range. In turn, this indicates that the surface of 13X zeolite has a better affinity for CO_2 than that of Cu-BTC, thus confirming the results of the modeling process and suggesting that the aforementioned higher CO_2 adsorption capacity per unit mass of Cu-BTC primarily depends not on the interaction between the framework and gas molecules but rather on the higher specific surface area and pore volume that Cu-BTC shows in comparison with 13X zeolite.

In regard to the heterogeneity parameter n, it is practically equal to unity for Cu-BTC, which indicates a homogeneous adsorption system and suggests that for this material the Langmuir model could fit the experimental data quite well; on the other hand, the value of n for 13X is greater than 2, indicating a more pronounced heterogeneity in the adsorption process. As already mentioned in the comments on the experimental results, this difference presumably depends on the different nature of the interactions between CO_2 molecules and the inner micropore walls of the considered substrates. For CO_2 adsorption on 13X zeolite, it is interesting to note that this

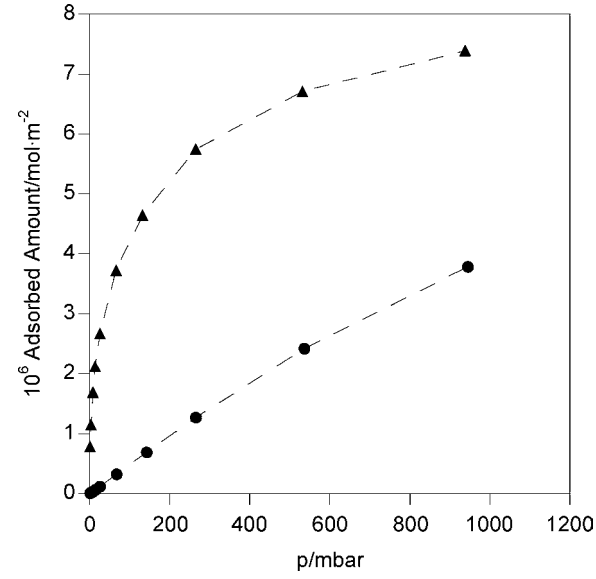

Figure 8. Adsorption isotherms of CO_2 at 293 K on synthesized Cu-BTC (●) and purchased 13X zeolite (▲) based on the surface areas of the adsorbents.

process partially develops through a chemical reaction that produces carbonate-like species starting from basic framework oxygen atoms and CO_2 molecules polarized by neighboring Na^+ ions.[31]

The value of the isosteric heat of CO_2 adsorption on Cu-BTC (25.9 kJ·mol^{-1}, as reported in Table 1) is about 20 % lower than that for CO_2 adsorption on 13X (about 32.5 kJ·mol^{-1}, as reported in Table 2). Such results are independent of the adsorbent fractional coverage because the expression for isosteric heat of adsorption derived from the Sips model reduces to the constant Q when the hypothesis of the temperature independence of the heterogeneity parameter n is taken into account.[30] Comparison of the calculated values of Q with the average values of the isosteric heat of adsorption for CO_2 that were experimentally determined and reported in previous papers[18,32] (i.e., about 28 kJ·mol^{-1} for Cu-BTC and 36 kJ·mol^{-1} for 13X) shows a satisfactory agreement. Since fixed-bed adsorption is an essentially adiabatic operation, the isosteric heat of adsorption is responsible for the temperature rise during the process. Once the working pressure range is fixed, adsorbent materials used in fixed-bed adsorption processes usually tend to lose part of their adsorption capacity as the working temperature increases. For this reason, a lower isosteric heat of adsorption is preferable when selecting the adsorbents, and because the CO_2 isosteric heat of adsorption for Cu-BTC MOF is clearly lower than that for 13X zeolite, Cu-BTC should be a more efficient adsorbent than 13X zeolite in fixed-bed adsorption processes.

4. Conclusions

CO_2 adsorption on the Cu-BTC metal−organic framework was modeled with the aim of comparing the performance of this material with that of 13X zeolite, which is often used for this application.

Laboratory-synthesized Cu-BTC samples were characterized by means of X-ray diffraction, thermogravimetry, and microporosimetric analysis, which indicated that the samples possess high crystallinity and high specific surface area and pore volume and that they are thermally stable up to 550 K.

CO_2 adsorption isotherms on Cu-BTC were evaluated at T = (283, 293, 318, and 343) K for $p \leq 1$ bar. For comparison, CO_2 adsorption isotherms on samples of commercial 13X zeolite were also determined under the same experimental conditions. Additionally, the N_2 adsorption isotherms both on Cu-BTC and on 13X zeolite were determined at $T = 293$ K, again for $p \leq 1$ bar. The experimental data showed that both adsorbents possess a high selectivity toward CO_2; moreover, Cu-BTC was found to have a higher CO_2 adsorption capacity than 13X in the range of near-ambient temperatures. The semiempirical Sips model was used to describe the data obtained for both sorbents, and a good agreement between the model and the experimental results was obtained. The model and the experimental results indicated that Cu-BTC has a noticeably higher adsorption capacity toward CO_2 than 13X zeolite and that its isosteric heat of adsorption is lower, suggesting that Cu-BTC could be more suitable for fixed-bed adsorption applications than 13X.

Acknowledgment

The support of Dr. Luigi Sanguigno (Italian Institute of Technology) in the development of the Matlab code is gratefully acknowledged.

Literature Cited

(1) *Climate Change 2007: Synthesis Report. Contribution of Working Groups I, II and III to the Fourth Assessment Report of the Intergovernmental Panel on Climate Change*; Intergovernmental Panel on Climate Change: Geneva, 2008.
(2) Halmann, M. M.; Steinberg, M. *Greenhouse Gas Carbon Dioxide Mitigation: Science and Technology*; CRC Press: Boca Raton, FL, 1999.
(3) Rostrup-Nielsen, R. *Catalysis: Science and Technology*; Springer-Verlag: Berlin, 1985.
(4) Ruthven, D. M. *Principles of Adsorption and Adsorption Processes*; Wiley: New York, 1984.
(5) Siriwardane, R. V.; Shen, M. S.; Fisher, E. P.; Poston, J. A. Adsorption of CO_2 on Molecular Sieves and Activated Carbon. *Energy Fuels* **2001**, *15*, 279–284.
(6) Shen, S. C.; Chen, X.; Kawi, S. CO_2 Adsorption over Si-MCM-41 Materials Having Basic Sites Created by Postmodification with La_2O_3. *Langmuir* **2004**, *20*, 9130–9137.
(7) Macario, A.; Katovic, A.; Giordano, G.; Iucolano, F.; Caputo, D. Synthesis of mesoporous materials for carbon dioxide sequestration. *Microporous Mesoporous Mater.* **2005**, *81*, 139–147.
(8) Chaffee, A. L.; Delaney, S. W.; Knowles, G. P. Hybrid mesoporous materials for carbon dioxide separation. *Abstr. Pap.—Am. Chem. Soc.* **2002**, *223*, FUEL-076.
(9) Huang, H. Y.; Yang, R. T.; Chinn, D.; Munson, C. L. Amine-Grafted MCM-48 and Silica Xerogel as Superior Sorbents for Acidic Gas Removal from Natural Gas. *Ind. Eng. Chem. Res.* **2003**, *42*, 2427–2433.
(10) Chang, A. C. C.; Chuang, S. S. C.; Gray, M.; Soong, Y. In-Situ Infrared Study of CO_2 Adsorption on SBA-15 Grafted with γ-(Aminopropyl)triethoxysilane. *Energy Fuels* **2003**, *17*, 468–473.
(11) Hiyoshi, N.; Yogo, K.; Yashima, T. Adsorption of Carbon Dioxide on Amine Modified SBA-15 in the Presence of Water Vapor. *Chem. Lett.* **2004**, *33*, 510–511.
(12) Xu, X.; Song, C.; Andresen, J. M.; Miller, B. G.; Scaroni, A. W. Preparation and characterization of novel CO_2 "molecular basket" adsorbents based on polymer-modified mesoporous molecular sieve MCM-41. *Microporous Mesoporous Mater.* **2003**, *62*, 29–45.
(13) Gargiulo, N.; Caputo, D.; Colella, C. Preparation and characterization of polyethylenimine-modified mesoporous silicas as CO_2 sorbents. *Stud. Surf. Sci. Catal.* **2007**, *170*, 1938–1943.
(14) Férey, G.; Mellot-Draznieks, C.; Serre, C.; Millange, F.; Dutour, J.; Surblé, S.; Margiolaki, I. A Chromium Terephthalate-Based Solid with Unusually Large Pore Volumes and Surface Area. *Science* **2005**, *309*, 2040–2042.
(15) Millward, A. R.; Yaghi, O. M. Metal−Organic Frameworks with Exceptionally High Capacity for Storage of Carbon Dioxide at Room Temperature. *J. Am. Chem. Soc.* **2005**, *127*, 17998–17999.
(16) Bourrelly, S.; Llewellyn, P. L.; Serre, C.; Millange, F.; Loiseau, T.; Férey, G. Different Adsorption Behaviors of Methane and Carbon Dioxide in the Isotypic Nanoporous Metal Terephthalates MIL-53 and MIL-47. *J. Am. Chem. Soc.* **2005**, *127*, 13519–13521.
(17) Llewellyn, P. L.; Bourrelly, S.; Serre, C.; Filinchuk, Y.; Férey, G. How Hydration Drastically Improves Adsorption Selectivity for CO_2 over CH_4 in the Flexible Chromium Terephthalate MIL-53. *Angew. Chem., Int. Ed.* **2006**, *45*, 7751–7754.
(18) Wang, Q. M.; Shen, D.; Bulow, M.; Lau, M. L.; Deng, S.; Fitch, F. R.; Lemcoff, N. O.; Semanscin, J. Metallo-organic molecular sieve for gas separation and purification. *Microporous Mesoporous Mater.* **2002**, *55*, 217–230.
(19) Chowdhury, P.; Bikkina, C.; Meister, D.; Dreisbach, F.; Gumma, S. Comparison of adsorption isotherms on Cu-BTC metal organic frameworks synthesized from different routes. *Microporous Mesoporous Mater.* **2009**, *117*, 406–413.
(20) Liang, Z.; Marshall, M.; Chaffee, A. L. CO_2 Adsorption-Based Separation by Metal Organic Framework (Cu-BTC) versus Zeolite (13X). *Energy Fuels* **2009**, *23*, 2785–2789.
(21) Schlichte, K.; Kratzke, T.; Kaskel, S. Improved synthesis, thermal stability and catalytic properties of the metal−organic framework compound $Cu_3(BTC)_2$. *Microporous Mesoporous Mater.* **2004**, *73*, 81–88.
(22) Chui, S. S.-Y.; Lo, S. M.-F.; Charmant, J. P. H.; Orpen, A. G.; Williams, I. D. A Chemically Functionalizable Nanoporous Material $[Cu_3(TMA)_2(H_2O)_3]_n$. *Science* **1999**, *283*, 1148–1150.
(23) Mueller, U.; Schubert, M.; Teich, F.; Puetter, H.; Schierle-Arndt, K.; Pastre, J. Metal−organic frameworks—Prospective industrial applications. *J. Mater. Chem.* **2006**, *16*, 626–636.
(24) Sing, K. S. W.; Everett, D. H.; Haul, R. A. W.; Moscou, L.; Pierotti, R. A.; Rouquerol, J.; Siemieniewska, T. Reporting physisorption data for gas/solid systems with special reference to the determination of surface area and porosity. *Pure Appl. Chem.* **1985**, *57*, 603–619.
(25) Gregg, S. J.; Sing, K. S. W. *Adsorption, Surface Area, and Porosity*; Academic Press: London, 1982.
(26) Breck, D. W. *Zeolite Molecular Sieves: Structure, Chemistry and Use*; Wiley: New York, 1974.

(27) Jadhav, P. D.; Chatti, R. V.; Biniwale, R. B.; Labhsetwar, N. K.; Devotta, S.; Rayalu, S. S. Monoethanol Amine Modified Zeolite 13X for CO_2 Adsorption at Different Temperatures. *Energy Fuels* **2007**, *21*, 3555–3559.

(28) Vitillo, J. G.; Regli, L.; Chavan, S.; Ricchiardi, G.; Spoto, G.; Dietzel, P. D. C.; Bordiga, S.; Zecchina, A. Role of Exposed Metal Sites in Hydrogen Storage in MOFs. *J. Am. Chem. Soc.* **2008**, *130*, 8386–8396.

(29) Sips, R. On the Structure of a Catalyst Surface. *J. Chem. Phys.* **1948**, *16*, 490–495.

(30) Do, D. D. *Adsorption Analysis: Equilibria and Kinetics*; Imperial College Press: London, 1998.

(31) Martra, G.; Coluccia, S.; Davit, P.; Gianotti, E.; Marchese, L.; Tsuji, H.; Hattori, H. Acidic and basic sites in NaX and NaY faujasites investigated by NH_3, CO_2 and CO molecular probes. *Res. Chem. Intermed.* **1999**, *25*, 77–93.

(32) Chue, K. T.; Kim, J. N.; Yoo, Y. J.; Cho, S. H.; Yang, R. T. Comparison of Activated Carbon and Zeolite 13X for CO_2 Recovery from Flue Gas by Pressure Swing Adsorption. *Ind. Eng. Chem. Res.* **1995**, *34*, 591–598.

Received for review March 10, 2010. Accepted July 2, 2010.

JE1002225